

# DEVELOPMENT OF A FOLDED MAGIC TEE FOR THE ILC POWER DISTRIBUTION SYSTEM

Prakash Joshi<sup>a</sup>, Toshihiro Matsumoto<sup>a,b</sup>, Shinichiro Michizono<sup>a,b</sup>

<sup>a</sup>SOKENDAI (The Graduate University for Advanced Studies), 240-0193, Hayama, Japan

<sup>b</sup>KEK (High Energy Accelerator Research Organization), 305-0801, Tsukuba, Japan

## Abstract

The folded magic tee (FMT) is a component of the variable power divider (VPD). It is used in the radio frequency (RF) power distribution system of the International Linear Collider (ILC). A unique characteristic of this device is that the phase and coupling ratios can be adjusted. The fixed-phase shifter and U-bend with actuator are two other components of the VPD. The VPD is completed by assembling two FMTs, four fixed-phase shifters, and two U-bends. The FMT was designed and manufactured. Simulated and measured S parameters of the FMTs satisfy the requirements. Two FMTs were tested in an L-band 1.3 GHz resonant ring with a repetition rate of 5 Hz, where a maximum of 5.5 MW transmission is possible. The FMTs were pressurized to 0.2 MPa (29 psig) using nitrogen gas. The test was conducted by gradually increasing the power at various pulse widths.

## INTRODUCTION

The International Linear Collider (ILC) is a future electron-positron collider with a center of mass of energy 250 GeV and luminosity of  $1.35 \times 10^{34} \text{ cm}^{-2} \text{ s}^{-1}$  with the option to upgrade in the future [1]. According to the ILC-Technical Design Report (TDR) electrons and positrons are accelerated from 15 to 125 GeV in the opposite direction in the superconducting (SC) 9-cell 1.3 GHz tesla-type cavities of main linac [2]. The average accelerating gradient of the cavities is 31.5 MV/m with a variation of  $\pm 20\%$ . This has been addressed by adjusting the coupling ratio of the variable hybrid to  $\pm 25\%$  [3]. A 10 MW multibeam klystron drives 39 SC cavities through three local power distribution systems (LPDSs), as shown in Fig. 1. The 13 cavities of LPDS are grouped into three sub-LPDS. The first two sub-LPDSs contain four cavities and the final one has five cavities, as shown in Fig. 1. The klystron emits radio frequency (RF) power through two 5 MW ports that are distributed into three LPDSs using two 5 MW variable power dividers (VPDs). The use of 5 MW VPDs is now proposed instead of the 5 MW variable hybrid mentioned in ILC-TDR.

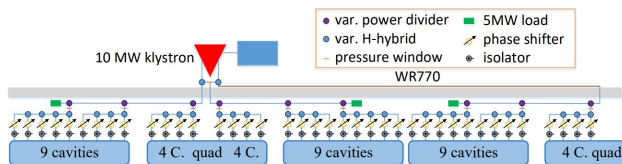


Figure 1: Power distribution system for the ILC [1].

A VPD is a four-port network that can adjust the coupling ratio and phase. This device can be pressurized to 0.2 MPa (29 psig), which is useful for power distribution in the pressurized waveguide system. Each VPD consists of two folded magic tees (FMTs), one on the input side and another on the output side. The FMT on the input side splits power equally into two ports of the collinear arm when the input is provided at the H-arm, as shown in Fig. 2. The FMT on the output side distributes RF power to the E- and H-arm according to the phase relationship between two inputs at its collinear arm.

## REQUIREMENTS

The FMT is a component of a VPD. Each VPD has two FMTs, as shown in Fig. 3. The return loss and isolated port losses at the H-arm and two ports of the collinear arm are less than -30 dB. The RF power is divided equally between two ports when input is provided at any port. The requirements of the 5 MW FMT are summarized in Table 1.

Table 1: Requirements of 5 MW Folded Magic Tee

| Parameters  | Value and Unit  |
|---|-----------------|
| RF power  | 5 MW            |
| Operational frequency   | 1.3 GHz         |
| Pulse width   | 1.65 ms         |
| Repetition rate   | 5 Hz            |
| N <sub>2</sub> gas pressure   | 0.2 MPa [4]     |
| Electric field  | < 3 MV/m        |
| $ S_{11} ,  S_{41} ,  S_{22} ,  S_{32} ,  S_{23} , \text{ and }  S_{33} $ | < -30 dB        |
| $ S_{21} ,  S_{31} ,  S_{12} ,  S_{42} ,  S_{13} , \text{ and }  S_{43} $ | -2.9 to -3.1 dB |

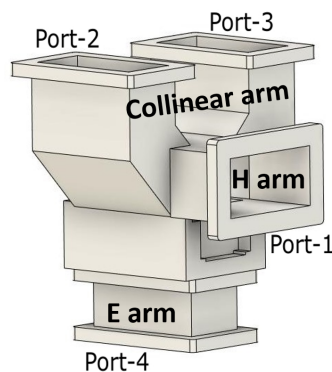


Figure 2: Descriptive design of a folded magic tee.

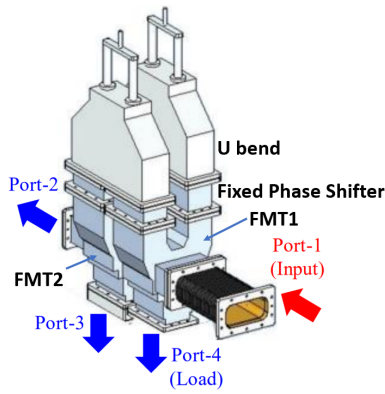


Figure 3: Descriptive design of a variable power divider [5].

In VPD, the RF power at port-2 ranges from 2.50 to 4.16 MW to satisfy the  $\pm 25\%$  variation in the coupling ratio of the variable hybrid.

## DESIGN AND SIMULATION

An FMT was designed and manufactured. The cross-sectional area of the E-arm was enlarged to suppress the electric field. Two posts of appropriate dimensions were installed such that the electric field remains below 3 MV/m and S parameters satisfied the requirements. To address the problem while installing the horizontal post, we prepared a separate E-arm and joined it to the main body. All four arm dimensions were designed such that bolts can be used from any direction to fix the arm with other components. The height, length, and width of FMT were 360, 250, and 330 mm respectively as shown in Fig. 4.

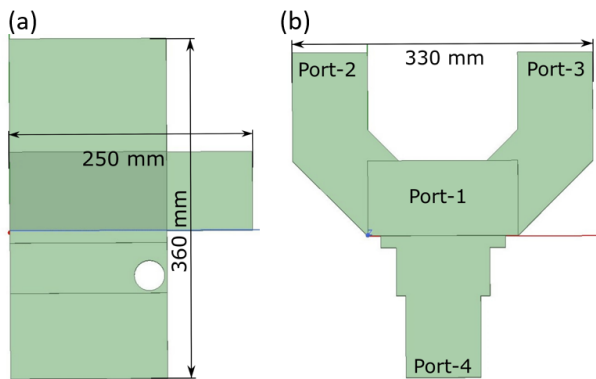


Figure 4: (a) Side view of the designed folded magic tee. (b) Front view of the designed folded magic tee.

The VPD was designed with a height, length, and width of 700, 580, and 330 mm respectively. The coupling ratio can be adjusted by sliding one U-bend inside the fixed phase shifter, and the phase can be adjusted by sliding both U-bends inside the fixed phase shifter in the same direction. When the heights of both U bends are the same, all power goes to port-2 and when height varies by 80 mm, then all power goes to port-3, as shown in Fig. 5. Figure 5 shows the

change in coupling ratio between port-2 and port-3 of the VPD with the difference in height between the two U-bends. The FMTs were tested in two optimal cases, as shown in Fig. 5. The U-bends and fixed phase shifters' dimensions were optimized to get the electric field below 3 MV/m. These two components remain to be manufactured.

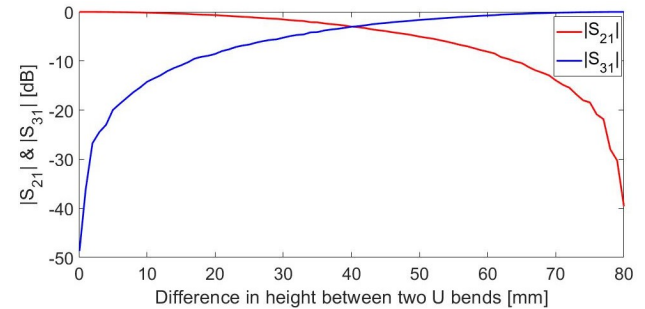


Figure 5: Change in coupling ratio between port-2 and port-3 in variable power divider owing to the difference in height between two U-bends. The S parameters  $|S_{11}|$  and  $|S_{41}|$  remains below -30 dB.

## TESTS

### Low Power Test

A low-power test of the two FMTs was conducted by using a four-port network analyzer. The return loss at port-1 of the FMT1 is close to -30.00 dB; therefore, it is used on the input side. In FMT1, port-1 is the input, and port-2 and port-3 are the outputs. In FMT2, port-2, and port-3 are inputs, and port-1 and port-4 are outputs. The S parameters almost satisfied the requirements listed in Table 2.

Table 2: Comparison among Required, Measured, and Simulated S-parameters of Folded Magic Tees

| S Para.    | Req. (dB)    | Sim. (dB) | Measured (dB) |        |
|------------|--------------|-----------|---------------|--------|
|            |              |           | FMT1          | FMT2   |
| $ S_{11} $ | < -30        | -43.01    | -29.63        | -27.83 |
| $ S_{21} $ | -2.9 to 3.1  | -3.01     | -3.06         | -3.04  |
| $ S_{31} $ | -2.9 to -3.1 | -3.01     | -3.06         | -3.06  |
| $ S_{41} $ | < -30        | -66.83    | -44.68        | -44.92 |
| $ S_{12} $ | -2.9 to -3.1 | -3.01     | -3.06         | -3.05  |
| $ S_{22} $ | < -30        | -42.10    | -36.09        | -33.67 |
| $ S_{32} $ | < -30        | -36.85    | -31.56        | -31.52 |
| $ S_{42} $ | -2.9 to -3.1 | -3.01     | -3.06         | -3.07  |
| $ S_{13} $ | -2.9 to -3.1 | -3.01     | -3.06         | -3.07  |
| $ S_{23} $ | < -30        | -36.86    | -30.96        | -30.99 |
| $ S_{33} $ | < -30        | -42.52    | -53.66        | -40.78 |
| $ S_{43} $ | -2.9 to -3.1 | -3.01     | -3.06         | -3.05  |

### High Power Test

**Resonant Ring:** It is a waveguide loop that can amplify the apparent power through the coupling of waves; therefore, it is useful for high-power tests. A four-port FMT can be

tested in the resonant ring (RR) by connecting the collinear arm of two FMTs with two H-corners to design a ring. A combination of two FMT and four H-corner functions as the VPD. When all power goes to port-1 of FMT2, it is the same scenario as when all power goes to port-2 of the VPD (setup1). Furthermore, when all power goes to port-4 of FMT2, it is similar to all power going to port-3 in the VPD (setup2). The coupling must be in the same phase as the ring power to amplify the power. A 3 dB hybrid with a phase shifter is used to increase the power gain by adjusting the phase [6], as shown in Fig. 6. The klystron output exhibits some fluctuation owing to the constant forward power with fluctuations in the gain. During the experiment, gain fluctuated between 10.8 to 13.8 dB owing to fluctuations in temperature.

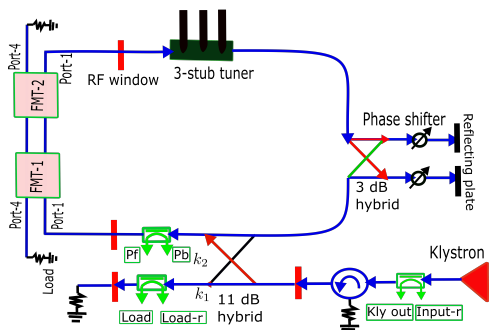


Figure 6: Sketch of the resonant ring showing two folded magic tees installed in it. The figure also shows the position of the components such as RF window, 3-stub tuner, klystron, directional couplers, circulator, phase shifter, 3 dB, and 11 dB hybrid.

For the high-power test, an L-band 1.3 GHz RR driven by an 800 kW klystron pulsed with a repetition rate of 5 Hz was used. A 500 kW circulator was used to prevent the klystron from reflecting power. The FMTs section of the ring was pressurized to 0.2 MPa (29 psig) using nitrogen gas, and the remaining section of the RR was pressurized to 0.1 MPa using  $SF_6$  gas. An RF window is utilized to apply distinct pressures and gases to the FMTs section and the remaining section of the ring, as shown in Fig. 6. A three-stub tuner was used to suppress the reflected power. Three directional couplers were installed to measure the RF power, as shown in Fig. 6. Five acoustic sensors and 16 temperature sensors were installed in the RR. The test was conducted for a pulse width of 50  $\mu s$ , 200  $\mu s$ , 500  $\mu s$ , 1.00 ms, and 1.65 ms. For each pulse, the RF power was increased gradually, but the test was not performed continuously; instead, it was conducted at a favorable time and data were combined.

**Folded Magic Tee Setup1:** The lengths of the connections between FMT1 and FMT2 are the same for both collinear arms, as shown in Fig. 7. Therefore, the input phases at port-2 and port-3 of FMT2 are the same, and all power went to port-1 of the FMT2, and port-4 ends with the load, as shown in Fig. 7. This setup is similar to a VPD when

all power is transferred to port-2 in VPD. For each pulse width, the power was gradually increased and maintained for one hour at 1, 2, 3, 4, 5, and 5.5 MW, as shown in Fig. 8.

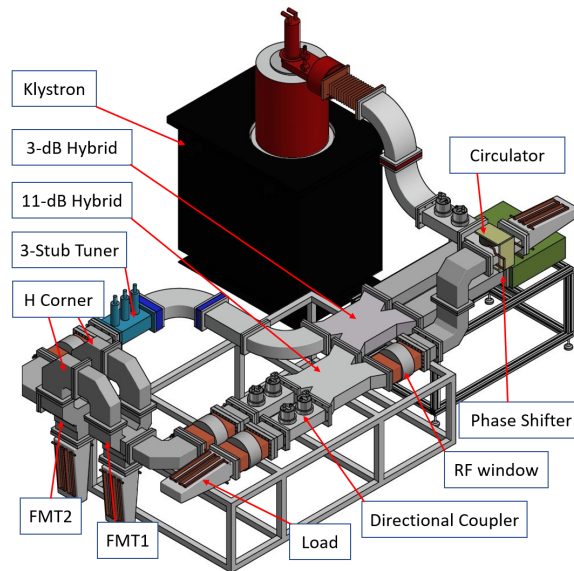


Figure 7: Setup1 showing the installation of two folded magic tees in a resonant ring for the high-power test. The component names are indicated in the figure.

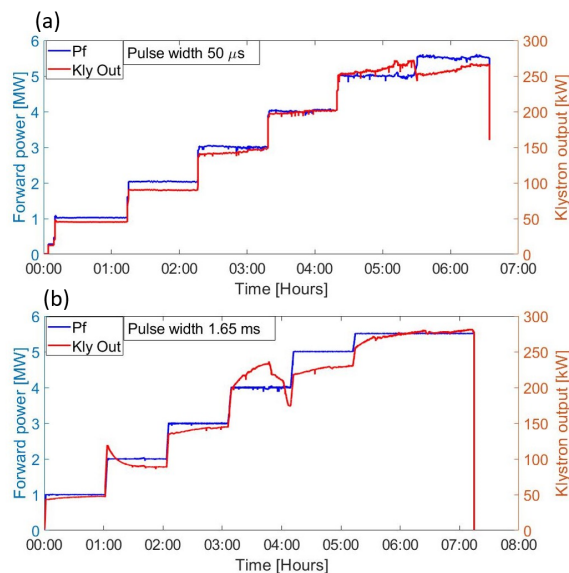


Figure 8: (a) One-hour testing of the folded magic tee at 1, 2, 3, 4, 5, and 5.5 MW with a pulse width of 50  $\mu s$ . (b) One-hour testing of the folded magic tee at 1, 2, 3, 4, 5, and 5.5 MW with a pulse width of 1.65 ms and an additional one hour at 5.5 MW. The fluctuation in klystron output was due to fluctuation in the gain.

**Folded Magic Tee Setup2:** The difference between the lengths of the connections between the collinear arms of FMT1 and FMT2 is 160 mm, as shown in Fig. 9. Therefore, the input phase at port-2 and port-3 of FMT2 are opposite,

and all power goes to port-4 of the FMT2 and port-1 ends with load, as shown in Fig. 9. This setup is similar to the VPD when all power is transferred to port-3 in the VPD. Our test plan was to repeat the process in Setup1. The first arcing was recorded in FMT1 at 3 MW for a pulse width of 200  $\mu$ s and solved through the conditioning effect. Owing to the arcing in the RR remaining test could not be completed.

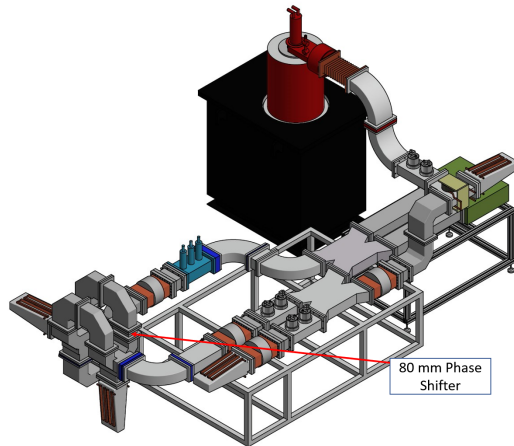


Figure 9: Setup2 for high-power test of the folded magic tee. The installation of an 80 mm phase shifter distinguished it from Setup1.

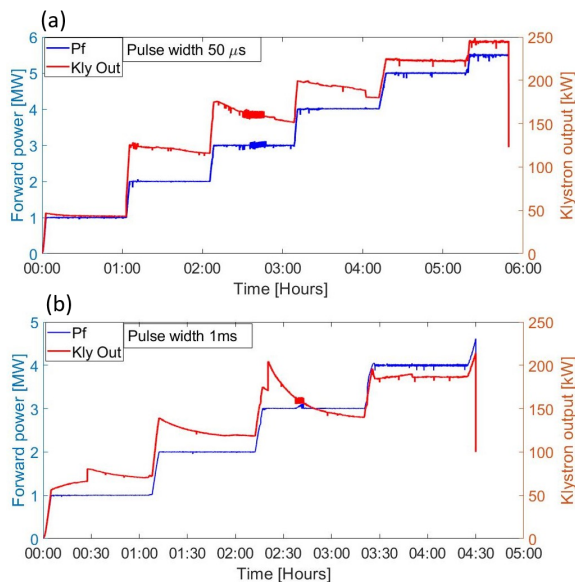


Figure 10: (a) One-hour testing of the folded magic tee at 1, 2, 3, 4, and 5 MW, and 30 min at 5.5 MW with a pulse width of 50  $\mu$ s. (b) One-hour testing at 1, 2, 3, and 4 MW with a pulse width of 1.00 ms. The fluctuation in the klystron output was due to fluctuation in the gain.

These two tests evaluate the reliability of the FMTs for the following reasons. In Setup1, the test was completed successfully at 5.5 MW, which is higher than the requirement of 5 MW. In Setup2, the test was completed for 4 MW with

a pulse width of 1.0 ms and 5.5 MW for 30 min with a pulse width of 50  $\mu$ s, as shown in Fig. 10. During operation, an average of 67% of power was transmitted to port-2, and 33% of power was transmitted to port-3 of the VPD. Therefore, Setup1 is more realistic.

Table 3: High-power Test Results

| Parameters         | Requirement | Test Setup1 |
|--------------------|-------------|-------------|
| RF power           | 5 MW        | 5.5 MW      |
| Pulse width        | 1.65 ms     | 1.65 ms     |
| Repetition rate    | 5 Hz        | 5 Hz        |
| $N_2$ gas pressure | 0.2 MPa     | 0.2 MPa     |

In the future, U-bends and fixed-phase shifters will be manufactured. The low- and high-power tests of the U-bends with fixed-phase shifters will be conducted. All three components will be assembled to construct VPD. Low- and high-power tests of the VPD will be conducted. Finally, 5 MW VPD will be demonstrated at the superconducting RF test facility of KEK.

## SUMMARY

Two folded magic tees were designed, manufactured, and tested. The low-power test was completed using a four-port network analyzer and the measured data were matched with requirements and simulation. The high-power test was completed in two test setups using a resonant ring. Test Setup1 offers a more realistic approach with variable power dividers. In Setup1 5.5 MW power with a pulse width of 1.65 ms was transmitted for two hours; therefore, the evaluated folded magic tees are suitable for use in a variable power divider.

## ACKNOWLEDGEMENTS

I am grateful to Kazuya Ishimoto, Naoto Numata, and Taiga Hanawa of the NAT group for their help with experiment setup and measurements. I also extend my thanks to Mizukoshi Corporation for manufacturing.

## REFERENCES

- [1] Lyn Evans and Shinichiro Michizono, "The International Linear Collider Machine Staging Report", 2017.
- [2] ILC, <https://linearcollider.org>
- [3] B. Du, T. Matsumoto, S. Michizono *et al.*, "Development of a compact Local Power Distribution System for the ILC", *Nuclear Instruments and Methods in Physics Research Section A*, 2020.
- [4] Faya Wang *et al.*, "Study of radio frequency breakdown in pressurized L-band waveguide for the ILC", *Applied Physics Letters*, 2013.
- [5] Nantista Christopher *et al.*, "Waveguide component R&D for the ILC", *Proceeding IPAC-2013*.
- [6] Du Baiting, "Development of a compact Local Power Distribution System for the ILC", *Ph.D. Thesis, SOKENDAI, Japan*, 2020.